Available online at www.sciencedirect.com
SCIENCE DIRECT®

Journal of the European Ceramic Society 24 (2004) 1389–1398

www.elsevier.com/locate/jeurceramsoc

Mesoporous semiconducting oxides for gas sensor application

Yasuhiro Shimizu*, Takeo Hyodo, Makoto Egashira

Department of Materials Science and Engineering, Faculty of Engineering, Nagasaki University, 1-14 Bunkyo-machi, Nagasaki 852-8521, Japan

Abstract

A fabrication procedure of thermally stable mesoporous SnO_2 and TiO_2 powders has been overviewed along with their gas-sensing properties. Treatment of an as-prepared composite material of a supramolecule surfactant and SnO_2, i.e. a self-assembly of the surfactant fringed with a SnO_2 thin wall, with phosphoric acid enabled us to fabricate thermally stable ordered mesoporous SnO_2 powder having a d_{100} value of 3.2 nm, a crystallite size of 2.0 nm and a large specific surface area of 305 $m^2\ g^{-1}$ even after calcination at 600 °C for 5 h. A thick film sensor fabricated with the ordered mesoporous SnO_2 powder exhibited higher sensing performance than that fabricated with SnO_2 powder prepared by a conventional method and therefore having a lower specific surface area. Surface modification of the conventional SnO_2 powder with a mesoporous SnO_2 layer was also found to be effective for improving the sensing properties. Mesoporous TiO_2 powder could be prepared by employing a modified sol-gel method with $Ti(NO_3)_4$ and polyethylene glycol having different molecular weights. Higher sensitivity was achieved with a disc-type sensor fabricated with mesoporous TiO_2 powder, in comparison with one fabricated with commercially available TiO_2 powder in the same form, but its sensing properties needed to be further modified.

Keywords: Mesoporous ceramics; Nanostructure; Semiconductor gas sensor; SnO_2; TiO_2

1. Introduction

Great emphasis is being given to nanostructured semiconducting metal oxides as a sensor material,[1–4] since grain-size reduction[5,6] and gas-diffusion control[7,8] have been proved to be useful for improving the gas-sensing properties. Sensitivity enhancement by grain-size reduction is pronounced when the grain-size of semiconducting metal oxides becomes smaller than the space-charge depth developed by surface chemisorbed oxygen species.[5,6] Sensitivity can also be enhanced by designing the specific pore structure of the sensing and/or over-coating layers or by employing nano-sized materials, so that diffusion of oxygen gas into the innermost region of the sensing layer, where a pair of electrodes is located, is restricted compared with that of gases of interest.[9]

Nano-sized semiconducting metal oxides have been prepared by a variety of methods, such as wet-chemistry,[2,3,10] microwave- or laser-assisted wet-chemistry,[4,11] physical-vapor-deposition[12] etc., and their advantages as a sensor material have been demonstrated extensively. High sensitivity can be achieved relatively easily with nano-sized sensor materials at their initial operation, but stabilization of their nanostructure, i.e., restriction of grain growth or aggregation of the nano-sized particles, during long-term operation at elevated temperatures is of primary importance for practical applications. Unfortunately, however, only a limited number of studies have been directed to fabricating thermally stable nano-sized sensor materials, while the hydrothermal treatment of tin oxide gel[10] and the addition of Ta, Nb[13] or Fe[12] to titania were reported to be effective for inhibiting the grain growth on calcination.

Mesoporous metal oxides are characterized with well-controlled mesoporous structure (pores are less than several tens of nm in diameter), in addition to their characteristics of nano-sized crystallites or particles and extremely high specific surface area.[14,15] Therefore, if mesoporous semiconducting oxides would be thermally stable enough, they may offer superior advantages, in comparison with merely nano-sized materials, in controlling the gas-diffusion process in sensors and in turn achieving tailored and more excellent gas sensing properties.

* Corresponding author. Tel.: +81-95-819-2644; fax: +81-95-819-2643.
E-mail address: shimizu@net.nagasaki-u.ac.jp (Y. Shimizu).

0955-2219/$ - see front matter © 2003 Elsevier Ltd. All rights reserved.
doi:10.1016/S0955-2219(03)00511-9

In this paper, some examples of thermally stable mesoporous sensor materials developed recently in our laboratory are overviewed along with their sensing performance. Our efforts have been focused on the preparation of thermally stable mesoporous powders aiming at expanding their application fields, and sensors were fabricated in a thick-film or sintered-disc type with these powders, though direct preparation of mesoporous films is another interesting approach.[16]

2. Gas-sensing properties of thermally stable mesoporous SnO_2

After the successful fabrication of mesoporous silica by utilizing a self-assembly of supramolecules, such as MCM (Mobil Composition of Matter) and SBA (Santa Barbara) families, numerous efforts have been directed to preparing mesoporous SnO_2,[14,15] which is one of the typical semiconductor gas sensor materials. However, the ordered mesoporous SnO_2 powders prepared so far are not always thermally stable and the poor thermal stability restricts their application fields, especially as semiconductor gas sensor materials have to be operated at elevated temperatures.

Recently, we have succeeded in preparing ordered mesoporous SnO_2 having sufficient thermal stability: a d_{100} value of 3.2 nm, a crystalline size of 2.0 nm and a large specific surface area of 305 $m^2\ g^{-1}$ were held even after calcination at 600 °C for 5 h in air.[17,18] The key procedure for maintaining the ordered mesoporous SnO_2 structure up to elevated temperatures is the treatment of the as-prepared powder with phosphoric acid (PA) prior to calcination. A preferable preparation procedure of the thermally stable ordered mesoporous SnO_2 powder is as follows. An assembly of a supramolecule surfactant fringed with a SnO_2 thin wall could be obtained from an aqueous solution dissolving a 2.0 wt.% of *n*-cetylpyridinium ($C_{16}PyCl$) as a surfactant and $Na_2SnO_33H_2O$ as a Sn-source at a molar ratio of $[C1_6PyCl]/[Na_2SnO_33H_2O] = 2.0$, after the pH of the solution was adjusted to 10 by adding a 35 wt.% HCl aqueous solution. The filtered product was then treated in a phosphoric acid (PA, 0.1 mol dm^{-3}) solution for about 2 h prior to calcination to remove the surfactant. Addition of mesitylene (trimethylbenzene, MES) to the precursor solution at a molar ratio of $[MES]/[Na_2SnO_33H_2O] = 2.5$ was also found to be effective for improving the thermal stability.

The usefulness of the PA treatment and the MES addition can be confirmed by the XRD patterns of the resultant powders before and after calcination, as shown in Fig. 1. Here, PA/m-SnO_2 and PA/m-SnO_2(MES) represent the powders prepared with and without MES in the precursor solution, respectively and then treated with PA, while m-SnO_2 stands for the powder prepared without MES and PA. The appearance of a peak around $2\theta \approx 2°$, assigned to a 100 diffraction peak, reveals that all the as-prepared powders are in a ordered mesoporous structure with a d_{100} value (corresponds to the distance between ordered SnO_2 walls) of about 4 nm. However, it is obvious that the ordered mesoporous structure of m-SnO_2 is fractured completely by calcination at 600 °C for 5 h in air, as shown in Fig. 1(a), indicating the poor thermal stability of m-SnO_2 prepared only by utilizing the self-assembly of a surfactant. In the case of m-SnO_2 powder, the SnO_2 crystallite size, calculated by Scherrer's equation based on XRD data in the range of 20–80°, increased markedly from 1.9 to 9.4 nm by the calcination. Thus, the growth of SnO_2 crystallite is considered to be responsible for the fracture of the ordered mesoporous structure. In contrast, the PA treatment is confirmed to be effective for improving the thermal stability of the ordered mesoporous structure, since the 100 diffraction peak appears even after calcination at 600 °C, as shown in Fig. 1(b). But, the diffraction peak shifts to a higher angle by the calcination, corresponding to a decrease in d_{100}-value from 4.1 to 3.2 nm. Furthermore, the addition of MES in the precursor solution is found to highlight the effect of the PA treatment in improving the

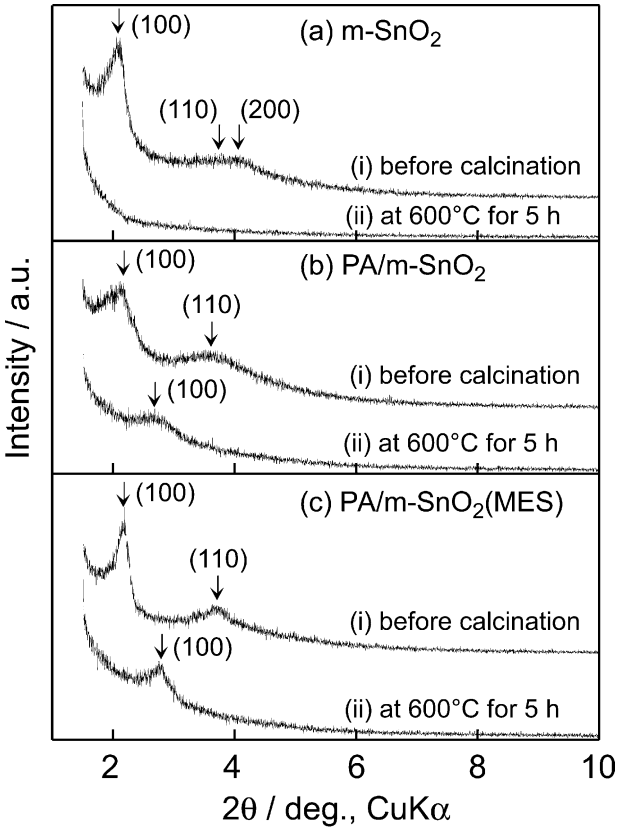

Fig. 1. XRD patterns of: (a) m-SnO_2; (b) PA/m-SnO_2; and (c) PA/m-SnO_2(MES) (preparation conditions: $C_{16}PyCl$ concentration = 2.0 wt.%, $[C_{16}PyCl]/[Na_2SnO_33H_2O] = 2.0$, $[MES]/[Na_2SnO_33H_2O] = 2.5$, pH = 10).

thermal stability, since a higher 100 peak appears after the calcination as shown in Fig. 1(c), although MES is reported in the literatures to be useful for stabilizing the micelle structure of the surfactant in the precursor solution and/or for the enlargement of the resulting mesopores.[19] The ordered mesoporous structure observed with as-precipitated m-SnO_2(MES) was also fractured completely after calcination at 600 °C for 5 h in air (the data in not shown here), indicating the uselessness of MES in enhancing the thermal stability of the ordered mesoporous structure. As for the PA/m-SnO_2 and PA/m-SnO_2(MES) powders, no change and only a slight change from 1.7 to 2.0 nm in crystallite size was induced by the calcination. Thus, the PA treatment is confirmed to be useful for reducing the growth of SnO_2 crystallites and then improving the thermal stability of the mesoporous structure.

Disappearance of the 110 peak after the calcinations, even for PA/m-SnO_2 and PA/m-SnO_2(MES) powders, is evidence for partial fracture of the ordered mesoporous structure. However, a TEM photograph of PA/m-SnO_2(MES) reveals that the ordered layer structure is maintained in almost all regions even after the calcination, as shown in Fig. 2(a). Owing to such an ordered mesoporous structure, the PA/m-SnO_2(MES) powder has a large pore volume at a pore diameter of about 1.6 nm with a large specific surface area of 305 $m^2\ g^{-1}$ even after calcination at 600 °C for 5 h. The mean pore diameter is comparable to the diameter of the ordered pores observed in Fig. 2(a). The difference between the d_{100}-value in Fig. 1(c) and the mean pore diameter is of course due to the SnO_2 wall parting the ordered mesopores. The thickness of the SnO_2 wall is calculated to be about 1.6 nm. Thus, the SnO_2 wall thickness is comparable to the SnO_2 crystallite size at a calcination temperature as high as 600 °C, indicating the suppression of three-dimensional crystallite growth with the PA treatment. The EDX analysis has revealed the existence of phosphorous atoms on the whole surface of PA/m-SnO_2(MES) particles after calcination at 600 °C, though the chemical and loading states have not been clarified yet. Some phosphorous compounds may be formed on the surface and/or at grain boundaries of SnO_2 crystallites during the calcination to suppress the growth of SnO_2 crystallites.

The ordered mesoporous structure was fractured partially by calcination at 700 °C [see Fig. 2(b)] and disappeared almost completely by calcination at 800 °C [see Fig. 2(c)]. In accordance with such a microstructural change, the crystallite size and the mean pore diameter of the resulting powder increased to 3.3 and 3.6 nm, respectively, after calcination at 800 °C. The specific surface area also decreased to 97.8 $m^2\ g^{-1}$ at 800 °C. However, this value is still large enough in comparison with those of m-SnO_2 (40.5 $m^2\ g^{-1}$) and c-SnO_2 (8.4 $m^2\ g^{-1}$, SnO_2 prepared from tin oxalate, a typical SnO_2 powder used for sensor fabrication by many researchers) calcined at 600 °C. Thus, PA/m-SnO_2(MES) is confirmed to have sufficient thermal stability for gas sensor application.

The PA/m-SnO_2(MES) powder calcined at 600 °C for 5 h was then used to fabricate a thick film-type sensor. The powder was mixed with an appropriate amount of a printing oil, which is composed of an alkyl ester of methacrylic acid as a binder, a toluene-based solvent, and an ammonium salt of polyacrylic acid as a plasticizer, in a manner similar to the procedure used in the

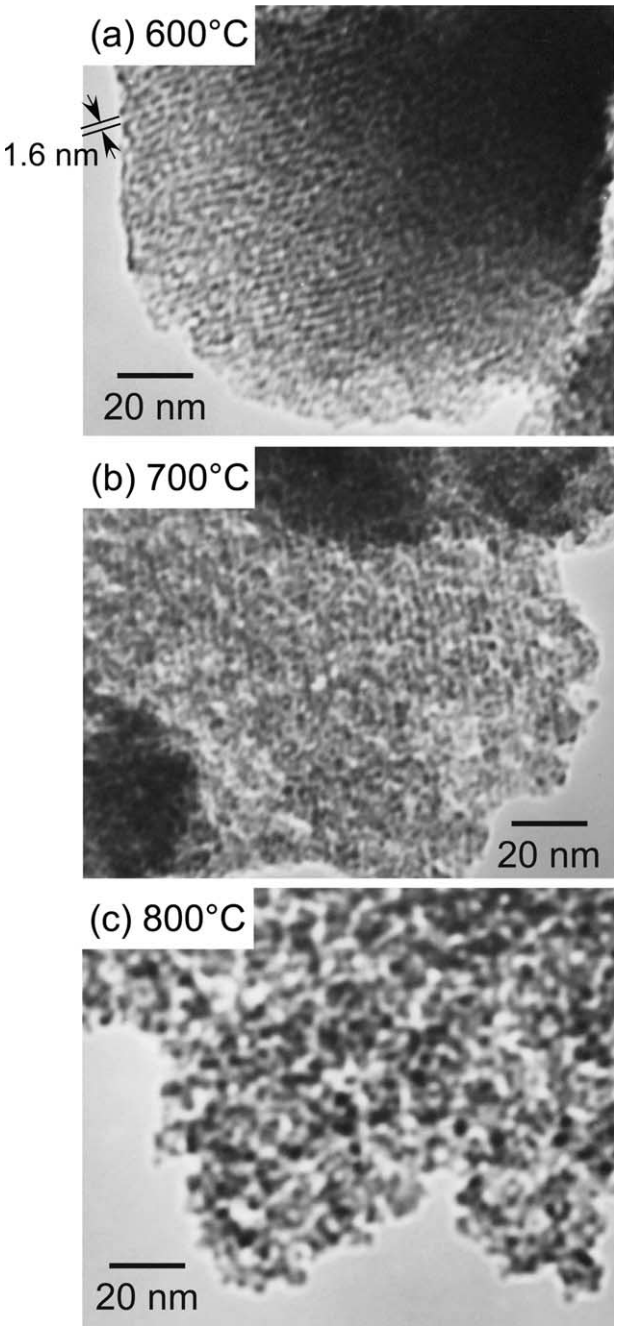

Fig. 2. TEM photographs of PA/m-SnO_2(MES) calcined at: (a) 600; (b) 700; and (c) 800 °C for 5 h in air.

slide-off transfer printing method,[20] and the resulting paste was screen printed on an alumina substrate, on which interdigitated Pt electrodes (gap between electrodes: 200 μm) had been printed. The printed film was subjected to heat treatment at 500 °C for 5 h in air prior to sensitivity measurement, and the sensor thickness was confirmed with SEM observation to be about 85 μm after the firing. Fig. 3 shows operating temperature dependence of the sensitivity of the PA/m-SnO_2(MES) thick film sensor to 500 ppm H_2. For comparative purposes, the result obtained with a c-SnO_2 thick film sensor (sensor thickness: 110 μm) fabricated in a similar manner as above is also depicted in the same figure. Here, sensitivity (k) is defined as the ratio (R_a/R_g) of sensor resistance in air (R_a) to that in 500 ppm H_2 balanced with air (R_g). The thick film sensor fabricated with thermally stable mesoporous SnO_2 powder exhibits higher H_2 sensitivity than the sensor fabricated with c-SnO_2 powder having a small specific surface area of 8.4 m^2 g^{-1}, the H_2 sensitivity of PA/m-SnO_2(MES) being six times as high as that of c-SnO_2 at 350 °C. The results shown in Fig. 3 demonstrate clearly the potential of the thermally stable mesoporous SnO_2 powder as a semiconductor gas sensor material. The resistance of the PA/m-SnO_2(MES) sensor in air was the order of 10^7 Ω at 350 °C and was higher than the c-SnO_2 sensor by more than three orders of magnitude under the same conditions, probably due to the small crystallite size of 2.0 nm. Since the depth of the space-charge region for pure SnO_2 is estimated to be about 3 nm in air at 300 °C,[5] the sensitivity enhancement by the grain-size reduction[5,6] can also be expected for the PA/m-SnO_2(MES) sensor. However, the H_2 sensitivity enhancement induced by the introduction of the ordered mesoporous structure in the SnO_2 powder is not so remarkable as expected from both the decrease in crystallite size and the increase in the specific surface area.

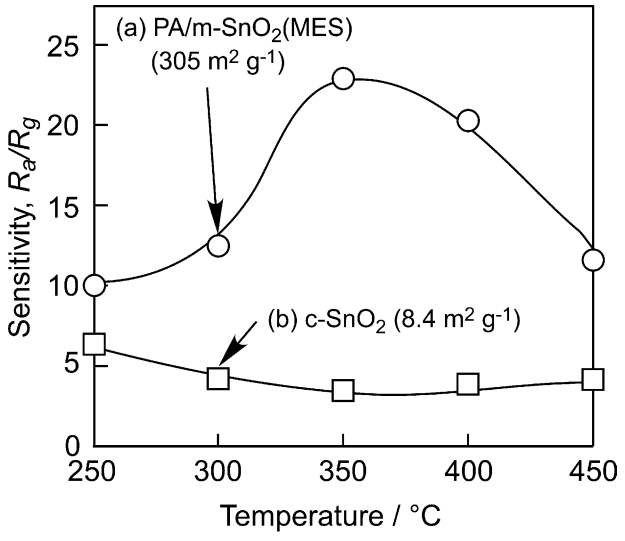

Fig. 3. Operating temperature dependence of sensitivity to 500 ppm H_2 of thick film sensors fabricated with PA/m-SnO_2(MES) and c-SnO_2 powders calcined at 600 °C.

The reason for the lower H_2 sensitivity than expected is probably due to the formation of large secondary particles in the case of PA/m-SnO_2(MES). Fig. 4 compares surface views between PA/m-SnO_2(MES) and c-SnO_2 sensors. The c-SnO_2 sensor consists of fine particles as shown in Fig. 4(b), in spite of the large crystallite size (34 nm) and the small specific surface area (8.4 m^2 g^{-1}) of the powder. In contrast, PA/m-SnO_2(MES) appears to form large secondary particles in the range of 2–5 μm as shown in Fig. 4(a), whereas its crystallite size is as small as 2.0 nm and the specific surface area is as large as 305 m^2 g^{-1}. It was found that such large secondary particles have already been formed in the as-precipitated products from the precursor solution. Thus, only the surface region of the secondary particles, especially the grain-boundaries among the secondary particles, may act as active sites for H_2 detection in the case of the PA/m-SnO_2(MES), whereas the particles consist of very fine SnO_2 crystallites and the ordered mesopores of 1.6 nm in diameter are well developed inside the particles. To prepare finer secondary particles and then to fully utilize the ordered mesoporous structure of PA/m-SnO_2(MES) powder as a gas sensor material, modification of preparation conditions is now under investigation.

3. Gas-sensing properties of conventional SnO_2 powder modified with a mesoporous SnO_2 thin layer

Chemical surface modification of SnO_2-based powders with ethoxysilanes has been proven to be useful for improving the gas-sensing properties to H_2 and hydrocarbons.[21] In these cases, the incorporated SiO_2 is considered to suppress the neck growth of SnO_2 grains during the final calcination to form thick film-type sensors and to lead to an increase in potential barrier height at SnO_2 grain-boundaries especially in air. The increased potential barrier height is assumed to be responsible for the sensitivity enhancement.

Surface modification of c-SnO_2 powder with a mesoporous SnO_2 thin layer, i.e. the use of the core-shell structure of a sensor material, is another interesting approach to improving the gas-sensing properties. This is because the resistance of the sensor fabricated with the modified powder in air can be controlled to be low at a practical level, due to the low resistance of core c-SnO_2, compared with the sensor employing only mesoporous SnO_2 powder, while the advantage of a mesoporous SnO_2 thin layer in detecting gases can be fully utilized in such a core-shell microstructure.

With the above idea in mind, the surface modification of c-SnO_2 powder with mesoporous SnO_2 was conducted in the following procedure.[22] c-SnO_2 was

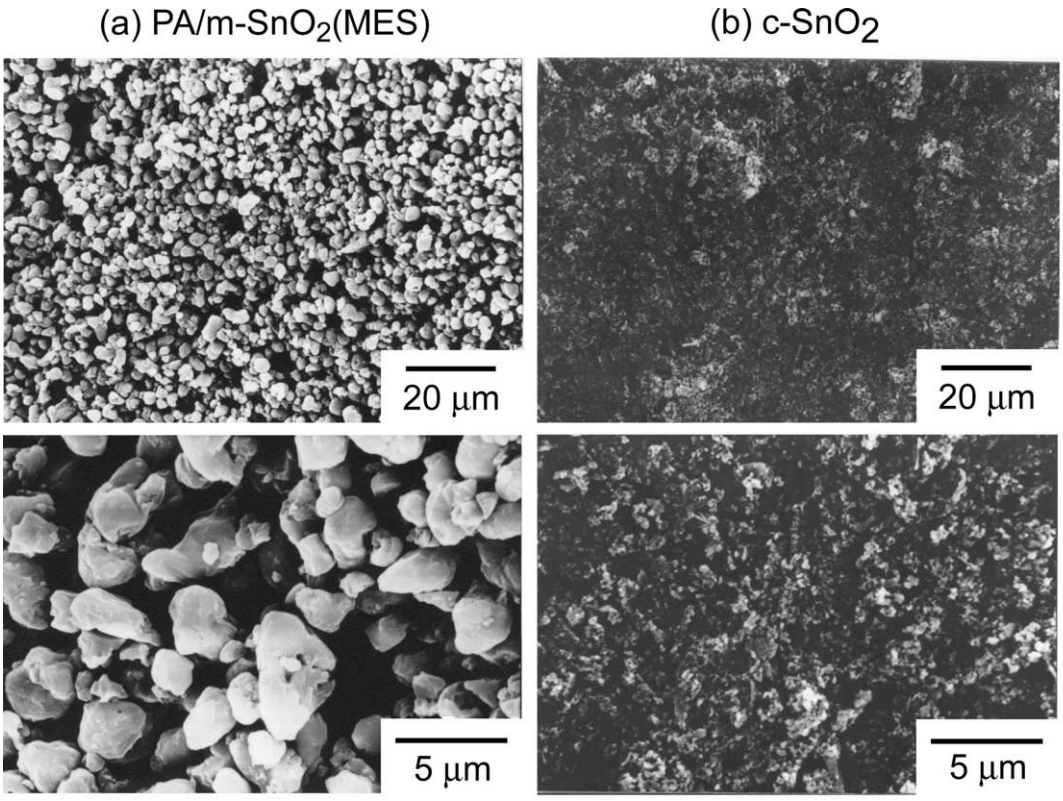

Fig. 4. SEM photographs of sensors fabricated with (a) PA/m-SnO_2(MES); and (b) c-SnO_2 powders calcined at 600 °C.

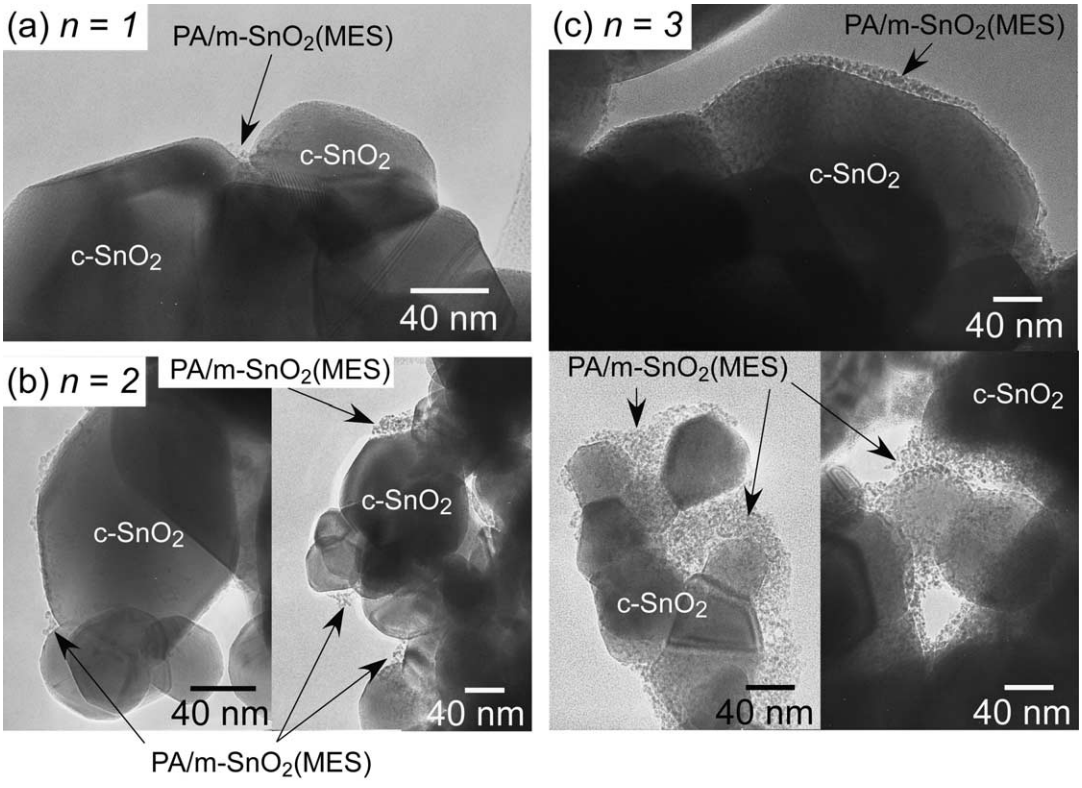

Fig. 5. TEM photographs of n\{PA/m-SnO_2(MES)\}/c-SnO_2 calcined at 600 °C for 5 h. (a) $n=1$, (b) $n=2$ and (c) $n=3$.

prepared from tin oxalate by calcination at 900 °C for 2 h. Two grams of c-SnO_2 powder was dispersed in 180 dm^3 of a 2.0 wt.% $C_{16}PyCl$ aqueous solution containing $Na_2SnO_33H_2O$ and MES at a molar ratio of $[C_{16}PyCl]/[Na_2SnO_33H_2O] = 2.0$ and $[MES]/[Na_2SnO_33H_2O] = 2.5$, respectively. The c-$SnO_2$ dispersed solution was outgassed under vacuum for a few minutes to achieve precipitation of a mesoporous SnO_2 thin layer on the c-SnO_2 surface. Thereafter the product was filtered off immediately under reduced pressure, and then was dried at 80 °C for 2 h. This cycle was repeated several times to achieve complete surface modification. In this case, the pH of the precursor solution was not intentionally adjusted. The resultant product was treated in a PA solution (0.1 mol dm^{-3}), and the filtered product was then subjected to calcination at 600 °C for 5 h in air. Hereafter, the powders thus prepared are referred to as n{PA/m-SnO_2(MES)}/c-SnO_2, where n represents the number of cycles for the modification with mesoporous SnO_2.

TEM photographs shown in Fig. 5 reveal that the surface of the c-SnO_2 particles can be covered almost completely with a PA/m-SnO_2(MES) thin layer after the three-times surface modification, while PA/m-SnO_2(MES) is likely to segregate at grain-boundaries with only single-time modification. However, no ordered mesoporous structure appears in the surface thin layer, as shown in Fig. 5(c), presenting a striking contrast to the PA/m-SnO_2(MES) powder shown in Fig. 2(a). Since c-SnO_2 powder is used as a core sensor material, formation of segregated secondary large particles is scarcely found by SEM observation (the photographs are not shown here). Although an ordered mesoporous structure was not visible in the TEM photographs, the volume of pores at a mean diameter of about 1.9 nm, corresponding to the ordered pores formed in the PA/m-SnO_2(MES) thin layer, clearly increased with increasing the number of surface modifications, as shown in Fig. 6. In accordance with this change, the specific surface area also increased from 5.34 (c-SnO_2) to 13.5 $m^2\ g^{-1}$ (3{PA/m-SnO_2(MES)}/c-SnO_2). These results imply that the surface modification of c-SnO_2 with a PA/m-SnO_2(MES) thin layer is successfully achieved, though the ordered mesoporous structure could not be developed in the thin layer under the present preparation procedure.

Fig. 7 shows response transients of thick film sensors fabricated with n{PA/m-SnO_2(MES)}/c-SnO_2 to 1000 ppm H_2 balanced with air at 400 °C and to 100 ppm NO and NO_2 balanced with air at 300 °C. These sensors were fabricated in the same manner as described above,

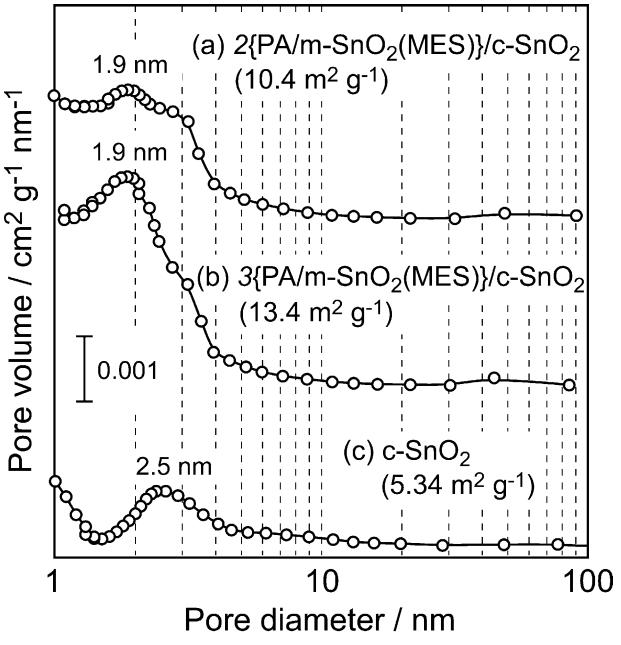

Fig. 6. Pore size distributions of: (a) 2{PA/m-SnO_2(MES)}/c-SnO_2; (b) 3{PA/m- SnO_2(MES)}/c-SnO_2; and (c) c-SnO_2.

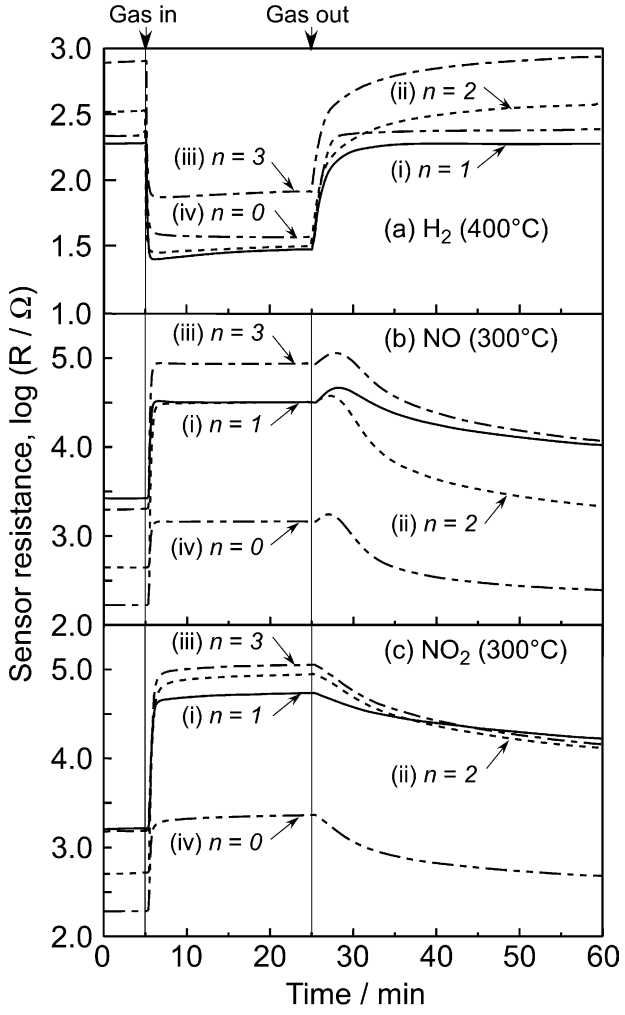

Fig. 7. Response transients of n{PA/m-SnO_2(MES)}/c-SnO_2 thick film sensors [n = (i) 1, (ii) 2, (iii) 3 and (iv) 0] to: (a) 1000 ppm H_2 balanced with air at 400 °C; (b) 100 ppm NO; (c) 100 ppm NO_2 balanced with air at 300 °C.

and the sensor thickness was in the range of 20–30 μm from SEM observation. For comparative purposes, the results obtained with a thick film c-SnO_2 sensor are also depicted in the same figure. Changes in sensor resistance in air induced by the surface modification with mesoporous SnO_2 are small as expected, and the sensor resistance is at a practical level even in NO_x atmosphere for all the sensors. It is obvious that all the n{PA/m-SnO_2(MES)}/c-SnO_2 sensors exhibit very quick responses to H_2 and relatively fast recovery, comparable to those of the c-SnO_2 sensor, as shown in Fig. 7(a). On the other hand, recovery of all the sensors is very slow after the removal of both NO and NO_2, indicating a low desorption speed of negatively-charged NO_x species chemisorbed strongly on the surface of PA/m-SnO_2(MES) and c-SnO_2 particles. Especially, the recovery after the removal of NO_2 is slowed down by the surface modification with mesoporous SnO_2, while a larger resistance increase upon exposure to NO_2 and hence higher sensitivity is induced by the surface modification, as shown in Fig. 7(c). An abnormal and slight increase in sensor resistance just after the removal of NO observed with all the sensors implies the formation of two kinds of NO adsorbates, i.e. weakly chemisorbed NO^+ and strongly chemisorbed NO^- species, under the present conditions, and reflects the difference in desorption behavior of these two adsorbates.

Variations in sensitivity induced by the surface modification with mesoporous SnO_2 are shown in Fig. 8. Here, the sensitivity to both NO and NO_2 is defined as R_g/R_a, since the sensor resistance increased upon exposure to these gases. As for the H_2 sensing properties, irrespective of the number of the surface modification cycle, the sensitivity enhancement is almost comparable among the three n{PA/m-SnO_2(MES)}/c-SnO_2 sensors and the temperature dependence of the sensitivity well resemble each other, as shown in Fig. 8(a). Namely, the magnitude of the sensitivity enhancement is not directly proportional to the amount of mesoporous SnO_2 covered on the c-SnO_2 particles and the maximum sensitivity appears in the temperature range 200–300 °C, while the sensitivity of c-SnO_2 increases monotonously with increasing the operating temperature up to 450 °C. These results imply that boundaries of c-SnO_2 particles dominate the H_2 sensitivity of n{PA/m-SnO_2(MES)}/c-SnO_2 sensors, and that mesoporous SnO_2 deposited especially on the grain-boundaries may act as a diffusion control layer for gaseous O_2 molecules. In other words, most of the mesoporous SnO_2 covering the surface of c-SnO_2 particles may not contribute to the enhancement of the H_2 sensitivity. In contrast, the sensitivities to both NO and NO_2 tend to increase with an increase in the number of surface modification cycles, and more pronounced enhancement is observed with NO_2 sensitivity, as shown in Fig. 8(b). Thus, the enhancement of NO_x sensitivities is almost correlated

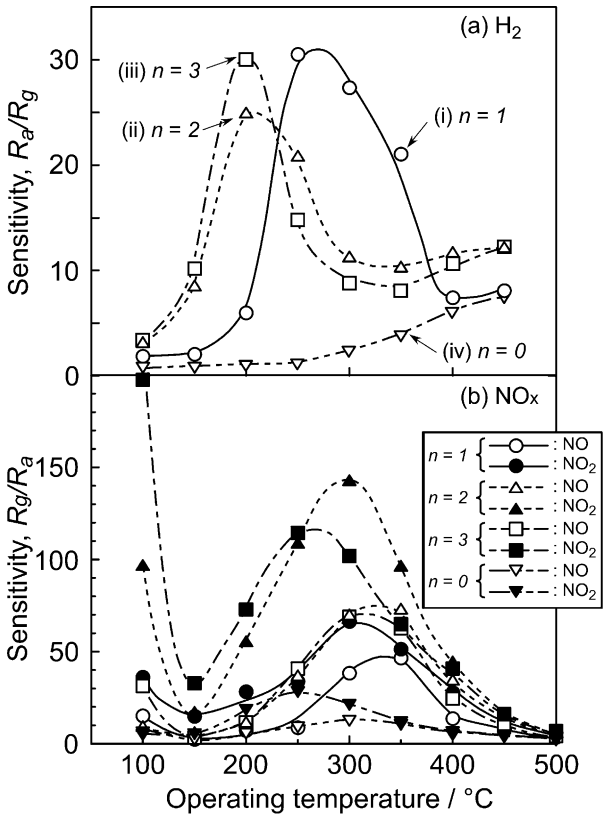

Fig. 8. Operating temperature dependence of sensitivities to 1000 ppm H_2, 100 ppm NO and 100 ppm NO_2 of n{PA/m-SnO_2(MES)}/c-SnO_2 thick film sensors.

with the amount of mesoporous SnO_2 deposited on the c-SnO_2 surface and then the specific surface area of n{PA/m-SnO_2(MES)}/c-SnO_2 sensors. In detecting NO_x, therefore, the mesoporous SnO_2 thin film may act as an adsorbent for NO_x gases and then dominate the sensitivities.

The above results demonstrate that the surface modification of c-SnO_2 powder with a mesoporous SnO_2 thin layer is an interesting approach to improvement and modification of the gas-sensing properties, though the mechanism for each gas should be studied in detail in future.

4. Gas-sensing properties of mesoporous TiO_2

The use of TiO_2 as a sensor material has been limited to O_2 sensors for automobile applications.[23] In this case, a resistance change induced by the reduction and oxidation of the oxide, i.e. a change in stoichiometry, is used as a sensor output, while reactivity of oxygen adsorbates toward combustible gases dominates the sensing properties of most semiconductor gas sensor materials, such as SnO_2, ZnO, WO_3 etc. However, recent progress in developing nanostructured TiO_2 powder offers its potential as a semiconductor gas

Table 1
Characterization of calcined TiO_2 powders prepared with PEG6000

Calcination temperature (°C)	Crystal phase	Surface area ($m^2\ g^{-1}$)	Pore volume ($cm^3\ g^{-1}$)	Crystallite size (nm)	Diameter of ordered mesopore (nm)
300	Anatase	265	0.12	3.7	4.1
400	Anatase	212	0.090	3.9	4.1
500	Anatase	88.9	0.050	9.0	4.1
600	Anatase	66.3	0.050	12.1	4.1
700	Rutile + anatase	3.0	0.0008	16.4	4.1

sensor material[12,13] operated at temperatures less than 500 °C, owing to an increased surface to volume ratio for the nanostructured powder and in turn an increased amount of reactive oxygen adsorbates.

Recently, we have prepared nano-sized and mesoporous TiO_2 powder by the same method as that reported by Liu et al.,[24] but with different molecular weights (MWs) of polyethylene glycol (PEG) as a dispersion and filming agent, and examined its thermal stability as well as gas sensing properties.[25] Mesoporous TiO_2 was prepared by the hydrolysis and condensation reaction of gel precipitates obtained from a mixture of $Ti(NO_3)_4$ and PEG with different MWs in aqueous solution and subsequent leaching out of PEG from the product in hot water.

Development of ordered mesoporous structure in the as-prepared TiO_2 powders can be confirmed by the low angle XRD patterns shown in Fig. 9. Namely, the appearance of a peak around $2\theta = 2.1°$ indicates the formation of an ordered mesoporous structure with a d_{100} value of ca. 4.1 nm for all the TiO_2 powders prepared. The peak intensity tends to increase with increasing the MW up to 4000, but decreased slightly at a MW of 6000. However, the TiO_2 powder prepared with PEG6000 had the largest specific surface area of 299 $m^2\ g^{-1}$ and the largest pore volume of 0.16 $cm^3\ g^{-1}$ with a crystallite of 3. 8 nm among the powders prepared. Therefore, thermal stability and gas-sensing properties of the TiO_2 powder prepared with PEG6000 (P6-TiO_2) were further examined below.

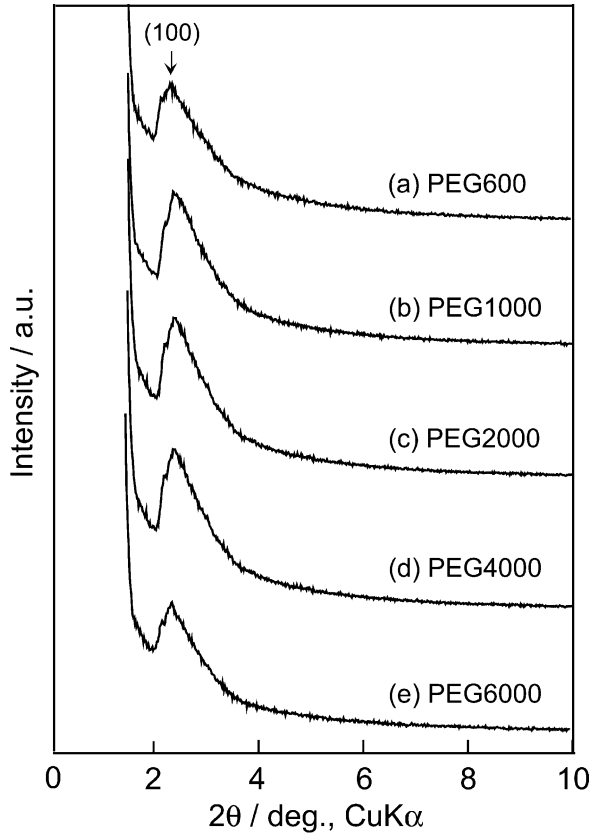

Fig. 9. Low angle XRD patterns of as-prepared TiO_2 powders by a modified sol-gel method with different molecular weights of PEG.

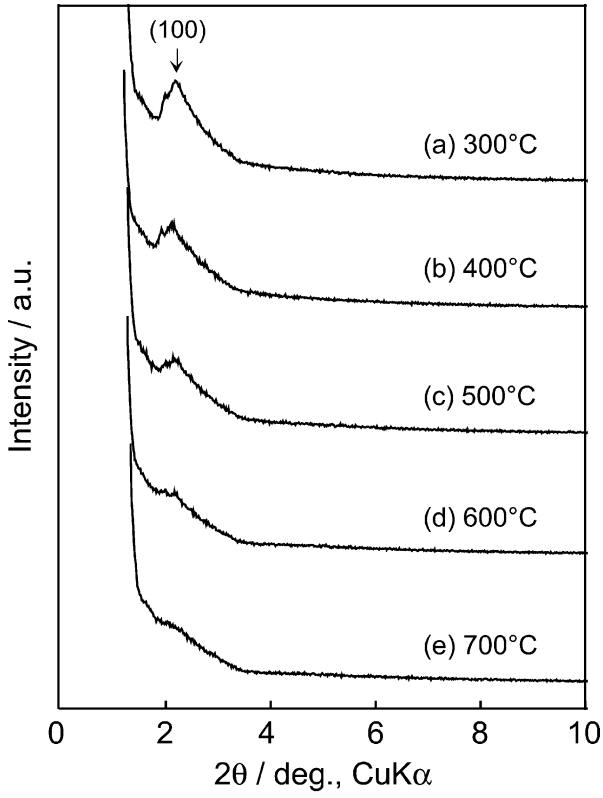

Fig. 10. Low angle XRD patterns of TiO_2 powder prepared with PEG6000 after calcination at elevated temperatures for 1 h in air.

Fig. 10 shows low angle XRD patterns of the P6-TiO_2 powders after calcination at elevated temperatures for 1 h in air. Microstructural data of the calcined P6-TiO_2 powders is summarized in Table 1. The intensity of the 100 diffraction peak decreases with increasing the calcination temperature as shown in Fig. 10, indicating partial destruction of the ordered mesoporous structure. However, the P6-TiO_2 powder calcined at 600 °C [P6-TiO_2(600)] still shows evidence, but with a very weak 100 diffraction peak, for the existence of the ordered mesoporous structure as shown in Fig. 10(d) and has a specific surface area of 66.3 $m^2\ g^{-1}$, which is seven times as high as that of commercially available TiO_2 powder (c-TiO_2, 9.7 $m^2\ g^{-1}$).

Owing to such a large surface area, the sensor fabricated with P6-TiO_2(600) powder (disc-type sensor fired at 550 °C for 3 h after pressing, 5.0 mmϕ, 0.5 mm thick) exhibited higher H_2 and CO sensitivities than the sensor fabricated with c-TiO_2 powder under the same conditions, as shown in Fig. 11. However, the sensitivities of the P6-TiO_2(600) sensor observed are small in comparison with those expected for other conventional SnO_2 and ZnO sensors, and therefore need to be further improved. In addition, the thermal stability of the P6-TiO_2 powder is found to be rather poor compared with that of PA/m-SnO_2(MES) described above. Thus, several approaches aimed at improving the thermal stability are now under investigation.

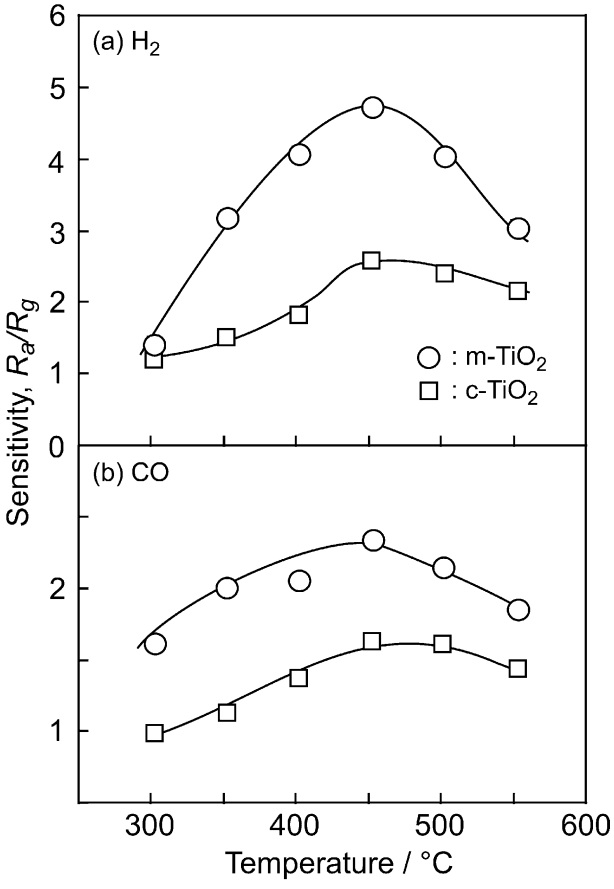

Fig. 11. Operating temperature dependence of sensitivities of TiO_2 sensors to: (a) 500 ppm H_2; and (b) 500 ppm CO balanced with air.

5. Conclusion

It was proved that gas-sensing properties of semiconductor gas sensors could be improved to a certain extent by controlling the meso- and nano-porous structure of the sensor materials. However, it is considered that the introduced meso- and nano-porous structure is not fully utilized for improving the sensing performance under the present fabrication conditions. Modification of fabrication conditions of the nanostructured semiconducting oxides is further encouraged for achieving greater sensing performance.

Acknowledgements

The present work was partly supported by Grant-in-Aid for Scientific Research (B) (No. 12450270 & 13555175) and for Young Scientists (A) (No. 14703015) from Japan Society for the Promotion of Science.

References

1. Traversa, E., Villanti, S., Gusmano, G., Aono, H. and Sadaoka, Y., Design of ceramic materials for chemical sensors: $SmFeO_3$ thick films sensitive to NO_2. *J. Am. Ceram. Soc.*, 1999, **82**, 2442–2450.
2. Martinelli, G., Carotta, M. C., Traversa, E. and Ghiotti, G., Thick-film gas sensors based on nano-sized semiconducting oxide powders. *MRS Bull*, 1999, **24**, 30–36.
3. Chiorino, A., Ghiotti, G., Prinetto, F., Carotta, M. C., Gnani, D. and Martinelli, G., Preparation and characterization of SnO_2 and MoO_x-SnO_2 nanosized powders for thick film gas sensors. *Sens. Actuators B*, 1999, **58**, 338–349.
4. Cirera, A., Vilà, A., Diéguez, A., Cabot, A., Cornet, A. and Morante, J. R., Microwave processing for low cost, mass production of undoped and in situ catalytic doped nanosized SnO_2 gas sensor powders. *Sens. Actuators B*, 2000, **64**, 65–69.
5. Xu, C., Tamaki, J., Miura, N. and Yamazoe, N., Relationship between gas sensitivity and microstructure of porous SnO_2. *Denki Kagaku (Presently, Electrochemistry)*, 1990, **58**, 1143–1148.
6. Xu, C., Tamaki, J., Miura, N. and Yamazoe, N., Grain size effects on gas sensitivity of porous SnO_2-based elements. *Sens. Actuators B*, 1991, **3**, 147–155.
7. Shimizu, Y., Nakamura, Y. and Egashira, M., Effects of diffusivity of hydrogen and oxygen through pores of thick film SnO_2-based sensors on their sensing properties. *Sens. Actuators B*, 1993, **13/14**, 128–131.
8. Shimizu, Y., Maekawa, T., Nakamura, Y. and Egashira, M., Effects of gas diffusivity and reactivity on sensing properties of thick film SnO_2-based sensors. *Sens. Actuators B*, 1998, **46**, 163–168.
9. Feng, C.-D., Shimizu, Y. and Egashira, X., Effect of gas diffusion process on sensing properties of SnO_2 thin-film sensors in a SiO_2/SnO_2 layer-built structure fabricated by sol-gel process. *J. Electrochem. Soc.*, 1994, **141**, 220–225.
10. Baik, N. S., Sakai, K., Miura, N. and Yamazoe, N., Hydrothermally treated sol solution of tin oxide for thin-film gas sensor. *Sens. Actuators B*, 2000, **63**, 74–79.

11. Cirera, A., Cabot, A., Cornet, A. and Morante, J. R., CO-CH_4 selectivity enhancement by in situ Pd-catalyzed microwave SnO_2 nanoparticles for gas detectors using active filter. *Sens. Actuators B*, 2001, **78**, 151–160.
12. Comini, E., Guidi, V., Frigeri, C., Riccò, I. and Sberveglieri, G., CO sensing properties of titanium and iron oxide nanosized thin films. *Sens. Actuators B*, 2001, **77**, 16–21.
13. Ferroni, M., Carotta, M. C., Guidi, V., Martinelli, G., Ronconi, F., Sacerdoti, M. and Traversa, E., Preparation and characterization of nanosized titania sensing film. *Sens. Actuators B*, 2001, **77**, 163–166.
14. Ulagappan, N. and Rao, C. N. R., Mesoporous phases based on SnO_2 and TiO_2. *Chem. Commun*., 1996, 1685–1686.
15. Severin, K. G., Abdel-Fattah, T. M. and Pinnavaia, T. J., Supramolecular assembly of mesostructured tin oxide. *Chem. Commun*., 1998, 1471–1472.
16. Grosso, D., Babonneau, F., Scanchez, C., Soler-Illia, G. J., de, A. A., Crepaldi, E. L., Albouy, P. A., Amenitsch, H., Balkenende, A. R. and Brunnet-Bruneau, A., A first insight in the mechanisms involved in the self-assembly of 2D-hexagonal templated SiO_2 and TiO_2 mesostructured films during dip-coating. *J. Sol-Gel Sci. Tech*., 2003, **26**, 561–565.
17. Hyodo, T., Nishida, N., Shimizu, Y. and Egashira, M., Preparation of thermally stable mesoporous tin dioxide powders with high specific surface area by utilizing self-assembly of surfactants. *J. Ceram. Soc. Jpn*, 2001, **109**, 481–483.
18. Hyodo, T., Nishida, N., Shimizu, Y. and Egashira, M., Preparation and gas-sensing properties of thermally stable mesoporous SnO_2. *Sens. Actuators B*, 2002, **83**, 209–215.
19. Huo, Q., Leon, R., Petroff, P. M. and Stucky, G. D., Mesostructure design with Gemini surfactants: Supercage formation in a three-dimensional hexagonal array. *Science*, 1995, **268**, 1324–1327.
20. Kawahara, A., Katsuki, H. and Egashira, M., Fabrication of semiconductor oxide thick films by slide-off transfer printing and their NO_2-sensing properties. *Sens. Actuators B*, 1998, **49**, 273–278.
21. Hyodo, T., Baba, Y., Wada, K., Shimizu, Y. and Egashira, M., Hydrogen sensing properties of SnO_2 varistors loaded with SiO_2 by surface chemical modification with diethoxydimethylsilane. *Sens. Actuators B*, 2000, **64**, 175–181.
22. Hyodo, T., Abe, S., Shimizu, Y. and Egashira, M., Preparation of thermally stable mesoporous SnO_2 for application to gas sensing material. *Chemical Sensors*, 2002, **18A**, 13–15 [in Japanese].
23. Tien, T. Y., Stadler, H. L., Gibbons, E. F. and Zacamnidis, P. J., TiO_2 as an air-to-fuel ratio sensor for automobile exhausts. *Ceram. Bull*, 1975, **54**, 280–282.
24. Liu, X., Yang, J., Wang, L., Yang, X., Lu, L. and Wang, X., An improvement on sol-gel method for preparing ultrafine and crystallized titania powder. *Mater. Sci. Eng*., 2000, **A289**, 241–245.
25. Devi, G. S., Hyodo, T., Shimizu, Y. and Egashira, M., Synthesis of mesoporous TiO_2-based powders and their gas-sensing properties. *Sens. Actuators B*, 2002, **87**, 122–129.